# A Technique for Constructing RTS Noise Model Based on Statistical Analysis

Cheng-Qing Wei[1,2,3], Yong-Zhong Xiong[2], Xing Zhou[1], Lap Chan[3]

[1]School of Electrical & Electronic Engineering, Nanyang Technological University
Nanyang Avenue, Singapore 639798, exzhou@ntu.edu.sg

[2] Institute of Microelectronics, Agency for Science, Technology and Research
11 Science Park Road, Science Park II, Singapore 117685, yongzhong@ime.a-star.edu.sg

[3]Chartered Semiconductor Manufacturing
60 Woodlands Industrial Park D, Street Two, Singapore 738406, chanlap@charteredsemi.com

## ABSTRACT

Low frequency noise such as random telegraph signal (RTS) noise is more and more important as device shrinks down. A significant part of the high frequency phase noise is generated due to up-converted low frequency noise. RF CMOS circuit performance and the device reliability will be limited and negatively impacted. Therefore, a noise model which accurately predicts the noise characteristics of deep-submicron devices is crucial for the low noise RFIC design. In this paper, the RTS noise parameters, i.e., pulse amplitude, pulse width and pulse delay, are obtained from the Schottky diode under different biases, and a technique for constructing the RTS noise model based on the statistical analysis of these noise data is introduced. From the comparisons of the noise data distributions, it is shown that the difference between the modeled RTS and measured RTS is quite small, and this model is useful in generating noise data because it is closely matched to the measured noise.

***Keywords***: random telegraph signal, low frequency noise, statistical noise model

## 1 INTRODUCTION

Throughout the last two decades, simple two-level random telegraph signals (RTS) have been observed in different types of devices, including reverse-biased diodes, bipolar junction transistors, junction field-effect transistors, and metal-oxide-semiconductor field-effect transistors (MOSFETs), etc. [1-3]. With device shrinking in dimensions, low-frequency noise is dominated by RTS noise. In the high-frequency regime, Schottky diodes with high speed advantage used in mixers and microwave oscillators have significant phase noise due to up-converted low frequency noise. This will negatively affect the circuit performance of analog and RF CMOS.

The Schottky diode used here is an n-doped Ti-Si Schottky diode with silicon doping density of $10^{18}cm^{-3}$. The total diode area is $0.67\mu m^2$ with $0.22\mu m^2$ contact area. The fabrication process is almost identical to the one proposed in [4, 5]. The standard noise measurement procedure was used at room temperature in a shielded room. The diode was connected to a battery-sourced voltage supply unit and to SR570 LN current preamplifier. The output was connected to a HP 35670A dynamic signal analyzer to collect the RTS noise signal in the time domain. The observed RTS noise pulse is from 0.48V to 0.68V in this study, and based on the statistical analysis, a RTS noise model is built with Matlab.

## 2 MEASUREMENT RESULTS AND DISCUSSIONS

Three parameters are needed to fully characterize one RTS pulse. They are pulse amplitude, pulse width and pulse delay. Hence, the RTS noise model in the time domain can be reconstructed if the statistical distributions of all three parameters are known for a particular bias. The details of the distribution of these three parameters at each bias are as follows:

Pulse amplitude distribution:
- 0.49V-0.57V: normal distribution
- 0.58V-0.68V: normal distribution with two peaks

Pulse width distribution:
- 0.49V-0.57V: lognormal distribution
- 0.58V-0.63V: lognormal distribution with two peaks
- 0.64V-0.68V: Gamma distribution

Pulse delay distribution:
- Exponential distribution for all biases

The normal distribution with single peak of pulse amplitude at lower bias is easy to be understood, because two-level RTS pulse is normally generated by a single active trap and each trap can capture only one electron, hence the magnitude of the current fluctuation due to a single trap should be the same, as indicated by the single peak in the amplitude distribution, while at higher biases, some high energy trap may be activated, leading to more peaks in the pulse amplitude distribution.

As shown in Fig.1, $T_A$ is the trap in silicon along the current flow path and $T_B$ is the trap at the interface near the Schottky contact. Since the electrons trapped at interface take much shorter path and less time to be recombined at Schottky contact compared to those trapped in silicon along the conduction path, the recombination rate of electrons

trapped by interface is higher than those trapped by silicon. Hence, it is easier for interface trapped electrons to be trapped or de-trapped, causing current fluctuation. Based on this understanding, at low biases, the lognormal distribution of the pulse width signifies the presence and dominance of interface traps that have smaller pulse width due to larger recombination rate. At larger biases, the current will increase and the current conduction path may widen and more silicon traps along the conduction path will be activated and contribute to the current fluctuation, which is reflected by the two-peak appearance in the lognormal distribution of pulse width from 0.58V to 0.63V. However, at very large bias, the electron trapped at the interface recombines too fast to be detected, so that current fluctuation due to interface trap can hardly be observed. In this situation, the current fluctuation is dominated by those traps in the silicon along the current flow path, hence, the observed Gamma distribution of pulse width from 0.64V to 0.68V. The exponential distribution of pulse delay within the whole bias range is also reasonable, since pulse delay time is closely related to the pulse width, given the fixed total record time length. The pulse delay time is basically very small in both lower bias and higher bias regions. In the lower bias region, this is due to the fast trapping-detrapping of interface traps dominated in this bias region, while in the higher bias region, it is due to the large pulse width of the silicon traps dominated in this bias region.

## 3 STATISTICAL MODEL DEVELOPMENT AND VERIFICATION

The RTS generator model built by Matlab Simulink is shown in Fig. 2, and this Simulink generator can generate random data for pulse amplitude, pulse width and pulse delay based on the respective statistical distribution assigned. The RTS noise reconstruction algorithm is as follows (see Fig. 3):

Step 1: RTS pulse amplitude (a randomly generated variable of a particular distribution) is generated at t=0, having a value of $c_1$ with the dimension of current.

Step 2: RTS pulse width (a randomly generated variable of a particular distribution) is generated at t=0, having a value of $a_1$ with the dimension of time.

Step 3: As time is increased, if the time elapsed is less than $a_1$, the signal keeps output as $c_1$.

Step 4: When the time elapsed is greater than $a_1$, a RTS pulse delay (a randomly generated variable of a particular distribution) having a value of $b_1$ with dimension of time is generated instantaneously.

Step 5: When the time elapsed is greater than $a_1$ but less than $a_1+b_1$, the signal keeps output as 0.

Step 6: When the time elapsed is greater than $a_1+b_1$, new random data for RTS pulse amplitude and pulse width having values of $c_2$ and $a_2$ respectively are generated again, based on their respective statistical distributions.

The simulation time period was set to 156.097ms, since for each set of data at each bias, the time record length is 7.8045ms, and total of 20 sets of data were taken for each bias. This loop continues until the end of the simulated period set. A comparison between the distributions of three parameters of the model generated RTS and measured RTS data needs to be done to check the model accuracy. As shown in Figs. 4-5, the distribution of the modeled RTS and measured RTS are nearly the same, the distribution type can be recognized as the same type and the difference of the mean and variance values are quite small between modeled RTS and measured RTS, respectively, thus this model can be used to simulate the RTS noise of this device. The frequency spectrum of measured RTS and modeled RTS can be found using Matlab code, which further proves the accuracy and usefulness of this model in generating noise spectrum which is closely matched to the FFT analysis of measured noise.

## 4 CONCLUSION

In this paper, a technique for constructing the RTS noise model based on the statistical analysis of the noise data obtained from the Schottky diode under different biases is introduced. The three RTS parameters: pulse amplitude, pulse width and pulse delay are very important, since the RTS noise model is built based on the statistical distributions of these three parameters. From the comparisons of the distributions, it is shown that the difference between the modeled RTS and measured RTS is quite small, and this model is useful in generating noise data because it is closely matched to the measured noise.

## REFERENCES


[1] Kirton MJ, *et al.*, "Noise in solid-state microstructures: a new perspective on individual defects, interface states, and low frequency noise," *Adv Phys*, Vol. 38, pp. 367, 1989.

[2] Hung KK, *et al.*, "Random telegraph noise of deep-submicrometer MOSFETs," *IEEE Electron Dev Lett*, Vol 11, pp. 90, 1990.

[3] Simoen E, *et al.*, "Explaining the amplitude of RTS noise in submicrometer MOSFETs," *IEEE Trans Electron Dev*, Vol 39, pp. 422, 1992.

[4] A. M. Cowley, *et al.*, "Titanium-silicon Schottky barrier diodes," *Solid State Electronics*, Vol 12, pp. 403-414, 1970.

[5] Y.Z. Xiong, G.Q. Lo, J.L. Shi, M.B. Yu, W.Y. Loh and D.L. Kwong, "Low-Frequency and RF Performance of Schottky-Diode for RFIC Applications and the Observation of RTS Noise Characteristics," accepted by 2006 NSTI Nanotechnology Conference and Trade Show, May 7-11, 2006, Boston, Massachusetts, U.S.A.

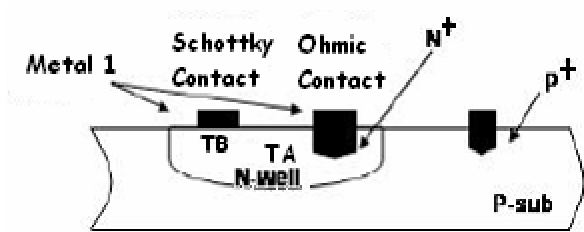


Figure 1: Side View of the Schottky Diode [4].

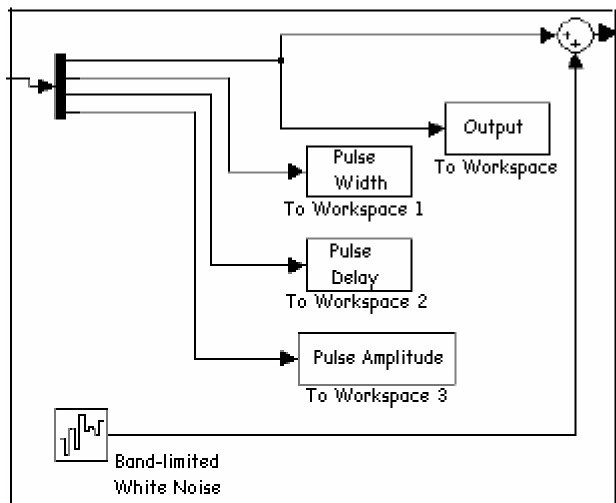


Figure 2: RTS Generator Model by Matlab Simulink.

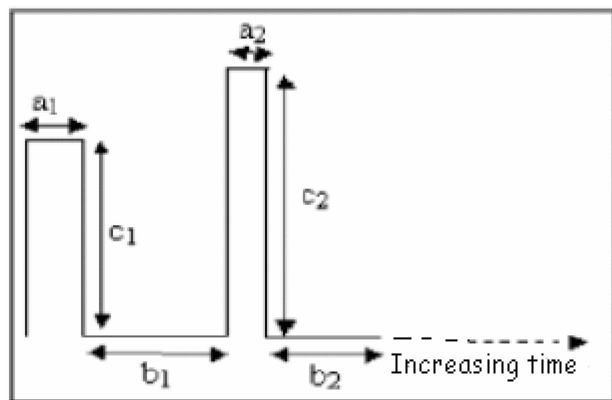


Figure 3: RTS Noise Reconstruction Algorithm.

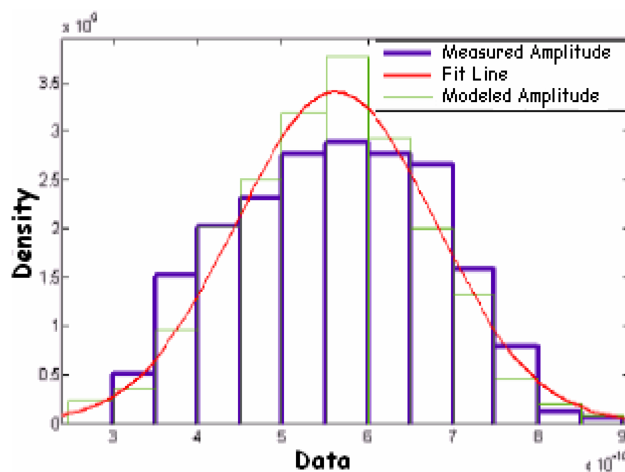


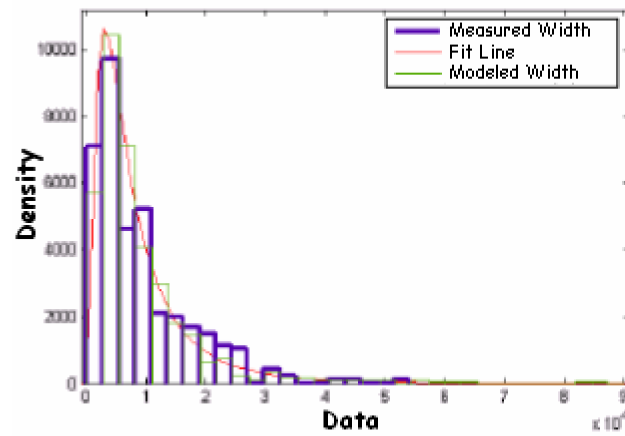


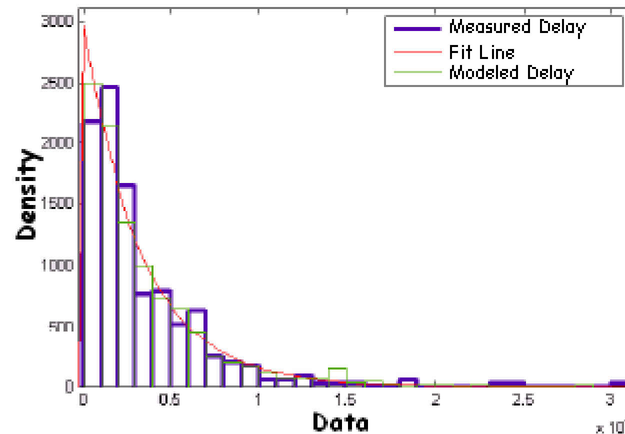


Figure 4: Comparison of the plot of three parameters between modeled RTS and Measured RTS.

**Amplitude** — Measured RTS

| | |
|---|---|
| Distribution: | Normal |
| Log likelihood: | 7592.85 |
| Domain: | -Inf < y < Inf |
| Mean: | 5.62524e-010 |
| Variance: | 1.37604e-020 |

Generated RTS

| | |
|---|---|
| Distribution: | Normal |
| Log likelihood: | 21506 |
| Domain: | -Inf < y < Inf |
| Mean: | 5.5747e-010 |
| Variance: | 1.22492e-020 |

**Pulse Width** — Measured RTS

| | |
|---|---|
| Distribution: | Lognormal |
| Log likelihood: | 2975.15 |
| Domain: | 0 < y < Inf |
| Mean: | 9.12436e-005 |
| Variance: | 9.18801e-009 |

Generated RTS

| | |
|---|---|
| Distribution: | Lognormal |
| Log likelihood: | 8447.68 |
| Domain: | 0 < y < Inf |
| Mean: | 8.82324e-005 |
| Variance: | 7.73223e-009 |

**Pulse Delay** — Measured RTS

| | |
|---|---|
| Distribution: | Exponential |
| Log likelihood: | 2554.06 |
| Domain: | 0 <= y < Inf |
| Mean: | 0.000336326 |
| Variance: | 1.13115e-007 |

Generated RTS

| | |
|---|---|
| Distribution: | Exponential |
| Log likelihood: | 6983.76 |
| Domain: | 0 <= y < Inf |
| Mean: | 0.000340956 |
| Variance: | 1.16251e-007 |

Figure 5: Statistical comparison of three parameters between modeled RTS and Measured RTS.